JOURNAL OF MATERIALS SCIENCE **34** (1999) 147–153

The influence of amount and type of additives on $\alpha \rightarrow \beta$ Si_3N_4 transformation

S. ORDOÑEZ
Departamento de Ingeniería Metalúrgica, Universidad de Santiago de Chile, Casilla de Correo 10233, Santiago, Chile
E-mail: sordonez@lauca.usach.cl

I. ITURRIZA, F. CASTRO
Centro de Estudios e Investigaciones Técnicas de Guipúzcoa, Manuel de Lardizabal 15 (20009) San Sebastián, España

During the liquid-phase sintering of silicon nitride-based ceramics, the dissolution of the Si_3N_4 is inferred from the tendency of the α-Si_3N_4 to transform to β-Si_3N_4. In order for this to correlate with densification it is necessary for the dissolved material to diffuse and precipitate, allowing contraction. In the present work the influence of the amount, quantity and type of additives on the $\alpha \rightarrow \beta$ transformation has been analysed. Two systems have been studied: Si_3N_4–SiO_2 and Si_3N_4–Y_2O_3–SiO_2. All samples were densified through hot isostatic pressing (HIP) of encapsulated compacts. In the Si_3N_4–SiO_2 system the dissolution of α-phase follows a zero-order kinetics and the amount of intergranular phase increases uniformly as a function of time, in this way eliminating dissolution as the rate-controlling mechanism in the transformation kinetic. In the Si_3N_4–Y_2O_3–SiO_2 system, the kinetics of dissolution are first-order and the amount of intergranular phase remains constant with time. This is a sufficient and necessary condition to establish that transformation in this system is a process whose kinetics are controlled by the dissolution of α-Si_3N_4 in the liquid phase.

1. Introduction

The densification of Si_3N_4 ceramics to densities close to the theoretical value has traditionally been carried out by liquid-phase sintering, both with and without the application of external pressure [1, 2]. Taking into account the amount of SiO_2 contained in the initial Si_3N_4 powder, sintering takes place in Si_3N_4–SiO_2–metallic oxide systems because of the liquid formed by reaction between SiO_2 and the oxide additions [3]. The compositional complexity of this liquid phase, combined with the associated $\alpha \rightarrow \beta$ transformation in the Si_3N_4 makes it difficult to identify unambiguously the basic material transport mechanisms involved and their relative importance during the process [4–6].

In an attempt to simplify this problem, the present work was carried out using SiO_2 as the sole addition, to study both the sintering and the transformation phenomena in silicon nitride. Additional samples, containing extra additions of Y_2O_3, were also prepared to study the influence of this additive on the transformation kinetics. This work has been complemented by X-ray diffraction (XRD) analysis, obtaining measurements with and without the use of an internal standard, and by microstructural observations using TEM.

2. Experimental procedure

The characteristics of the Si_3N_4 powders used in the present work are shown in Table I.

The additives used were yttria (∼99.9% pure) and precipitated silica of between 5 and 30 wt %. Theoretical density (TD) was calculated by the rule of mixtures using the initial compositions. The desired mixtures were prepared by dry milling for 48 h, using a ball mill consisting of a polyethylene container and silicon nitride milling media.

Green compacts were produced by cold isostatic pressing, applying a compaction pressure of 200 MPa, which resulted in compacts having densities of around 60% TD.

Before sintering, the compacts were coated using a borosilicate glass encapsulation method [7] and hot isostaticaly pressed within the temperature range 1700–1900 °C at an argon pressure of 150 MPa with several holding periods, using an ASEA-HIP press (QIH-6).

Density was measured by the Archimedes' principle. The characterization of the crystalline phases and $\alpha \rightarrow \beta$ transformation was carried out by X-ray diffractometry. Two quantitative methods have been used to determine the major crystalline phases: direct

TABLE I Composition (wt %), $\alpha/(\alpha+\beta)$ ratio and specific surface area of the Si_3N_4 powders

Powder	BET ($m^2\ g^{-1}$)	$\alpha/(\alpha+\beta)$	C	O	Fe	Al	Ca
H.Starck LC 12S	21.4	95.5	0.15	1.98	0.012	0.032	0.004
UBE SN-10	14	95	0.2	1.9	0.01	<0.005	<0.005

comparison using diffraction lines between 18° and 40° and the internal standard method using a constant amount of NiAL [8]. In this method, a calibration curve was first obtained using the original Si_3N_4 powders, and also α/β mixtures containing different amounts of pure β-Si_3N_4 plus 10% NiAI. The amount of vitreous phase was determined after measuring the absolute concentrations of all crystalline phases present by subtraction.

For microstructural analysis in the transmission electron microscope (TEM), discs were obtained from bulk specimens using a diamond cutting wheel to obtain sections ~0.5 mm thick, followed by a coring operation, using a 3 mm internal diameter diamond coring tool. The discs were mechanically ground to a thickness of about 0.1 mm, dimpled to ~50 μm and ion milled to electron transparency. A thin film of carbon was evaporated on the foils to avoid charging during exposure to the electron beam. Analysis was carried out using a Philips CM-12 scanning transmission electron microscope with a LaB_6 filament.

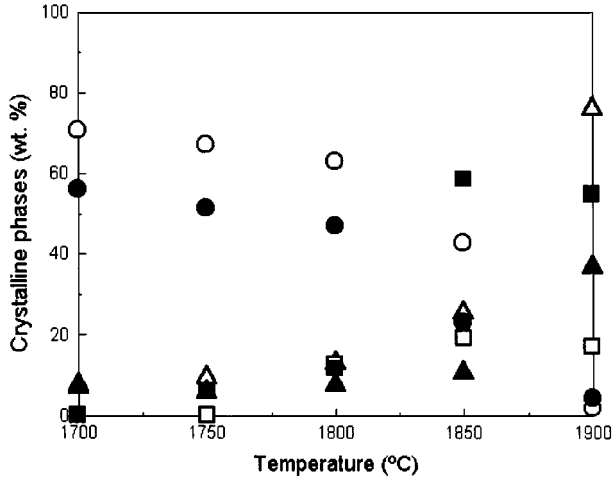

Figure 2 Weight fraction of the crystalline phases as function of sintering temperature for holding times of 60 min. (○, ●) α-Si_3N_4, (△, ▲) β-Si_3N_4, and (□, ■) Si_2N_2O. (○, △, □) Si_3N_4–10% SiO_2, (●, ▲, ■) Si_3N_4–20% SiO_2.

3. Results and discussion

Densification curves for Si_3N_4 mixed with increasing amounts of silica show different zones of the typical densification curves for a liquid-phase sintering process, depending on the additive content, and the temperature range studied (Fig 1).

The shape of these curves is analogous to that reported in earlier works for "pure" Si_3N_4 and $Si_3N_4 + Y_2O_3$ [9], although in the present case the range of temperatures for achieving full densification is narrower, possibly due to the larger amounts of liquid involved in sintering.

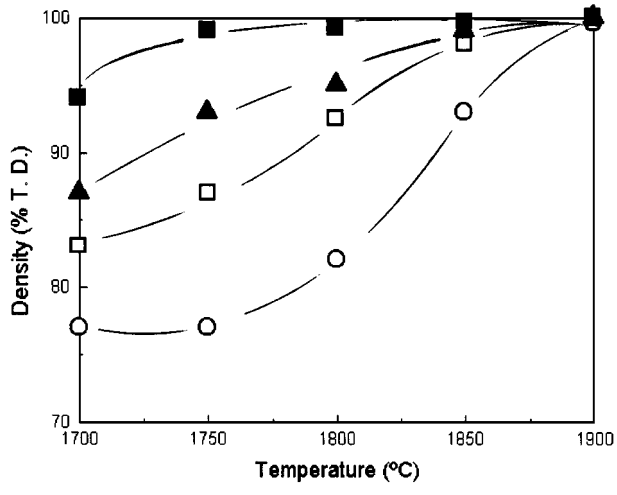

Figure 1 Dependence of the final density on temperature for SiO_2-doped silicon nitride. (○) 5% SiO_2, (□) 10% SiO_2, (▲) 15% SiO_2 and (■) 20% SiO_2.

As can be appreciated from Fig. 2, the densification of different $Si_3N_4 + SiO_2$ compositions, after HIPing for 1 h, is not accompanied by $\alpha \rightarrow \beta$ transformation up to a temperature of 1800 °C. Thus, such densities are thought to be reached without the intervention of dissolution–diffusion–precipitation mechanisms, because otherwise (assuming dissolved α-Si_3N_4 does not reprecipitate as α-Si_3N_4) β-Si_3N_4 and/or Si_2N_2O would have been detected.

If the amount of α-Si_3N_4 measured at temperatures below 1800 °C is observed to decrease for samples with increasing quantities of SiO_2, it seems clear that α-Si_3N_4 has dissolved in the silica without precipitating, giving a corresponding increase in the amount of available liquid during sintering. Mechanisms such as rearrangement, which gives rise to liquid redistribution to fill the porosity, are particularly important for large quantities of liquid phase and the lower end of the temperature range. Over 1800 °C, an additional contribution appears due to the diffusion–precipitation process and the consequent change in shape of the grains.

In samples containing 5% SiO_2 the mechanisms involved in the transformation, especially diffusion and precipitation, have a great influence on the densification. As a consequence of this, considerable increases in density are only obtained at temperatures for which a significant level of transformation is reached. The curves for densification and transformation of Si_3N_4–5% SiO_2 samples can be observed in Fig. 3.

For silica contents of 10% and 15%, the densification contribution from the dissolution–diffusion–precipitation mechanism is necessary to reach full density but, in contrast to the 5% SiO_2 composition, there

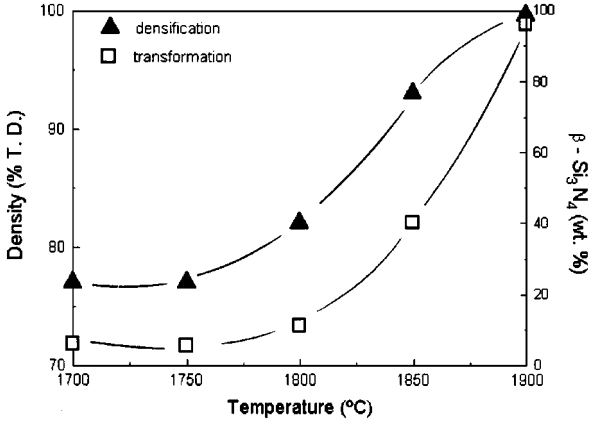

Figure 3 Influence of sintering temperature on the (□) transformation and (▲) densification of Si_3N_4–5% SiO_2.

is dissolution of α-Si_3N_4 in the liquid phase even at the lowest temperatures used.

In compositions with higher contents of SiO_2, rearrangement and porosity in-fill by the liquid are enough to reach densities close to the theoretical value; therefore complete densification occurs at temperatures in which transformation has not yet begun.

In the two extreme compositions analysed, it can be observed that for 5% SiO_2 full densification is reached only at 1900 °C with practically complete transformation (Fig. 3), while for 30% SiO_2, full density is obtained at 1700 °C, a temperature at which transformation has still not begun. It is evident, therefore, that by varying the silica content, dense samples can be obtained with different degrees of transformation. For compositions containing 10% and 20% SiO_2, the weight fractions of α-Si_3N_4 and β-Si_3N_4 measured showed that the quantity of vitreous phase for a given temperature was not constant with time, indicating that not all the α-Si_3N_4 dissolved in the liquid phase reprecipitates immediately as β-Si_3N_4 or Si_2N_2O. Fig. 4 shows the increase in the amount of vitreous phase with time for the $Si_3N_4 + 10\%$ SiO_2 sample.

At 1700, 1750 and 1800 °C, for both compositions, the quantity of α-Si_3N_4 dissolved in the liquid phase (either to be transformed into β-Si_3N_4, Si_2N_2O or

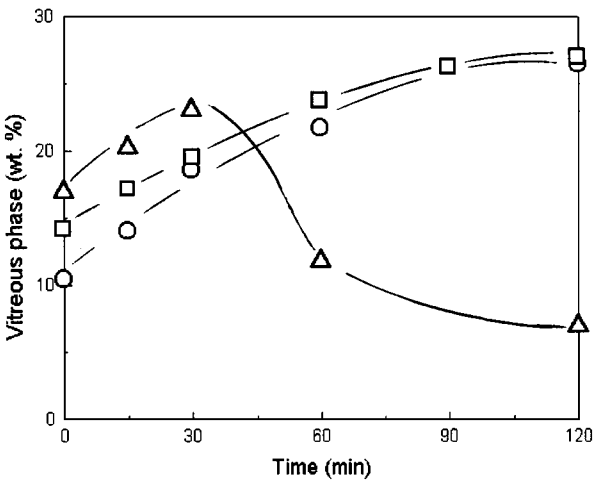

Figure 4 Evolution of the amount of vitreous phase with holding time for $Si_3N_4 + 10\%$ SiO_2. (○) 1700 °C, (□) 1750 °C and (△) 1800 °C.

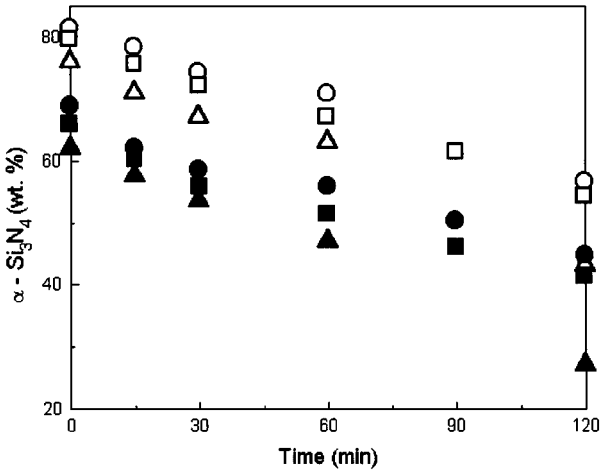

Figure 5 Linear relationship between α-Si_3N_4 and time, in samples of Si_3N_4–10% SiO_2 at (○) 1700 °C, (□) 1750 °C and (△) 1800 °C, and Si_3N_4–20% SiO_2 at (●) 1700 °C, (■) 1750 °C and (▲) 1800 °C.

remain in the intergranular phase) increases with time, with a constant dissolution rate; this can be expressed through the following equation

$$\frac{d\alpha}{dt} = -k \tag{1a}$$

which on integration gives

$$\alpha = \alpha_0 - kt \tag{1b}$$

The linear relationship between phase concentration and time can be seen in Fig. 5 for different sintering temperatures. This dependency indicates that the dissolution of α-phase, in the Si_3N_4-SiO_2 system, follows a zero-order reaction.

The quantity of intergranular phase is a function of time (Fig. 4) and this indicates that it is not the dissolution of the α-Si_3N_4 but the diffusion or precipitation process which controls the transformation kinetic in this system. Below 1850 °C the β-Si_3N_4 precipitation rate or the Si_2N_2O formation rate are less than the dissolution rate of the α-phase, and therefore the quantity of intergranular phase increases with time until all the α-Si_3N_4 has disappeared, or until the precipitation or formation rates overcome the phase dissolution rate. Between 1800 and 1850 °C, thermally activated processes, such as β-Si_3N_4 precipitation or Si_2N_2O formation, surpass their activation energy and although the dissolution of α-Si_3N_4 in the liquid phase will also be favoured, the β-phase precipitation and/or oxynitride formation rates exceed the dissolution rate with a consequent decrease of the quantity of vitreous phase.

If C is designated as the quantity of intergranular phase measured as vitreous phase at room temperature, this can be expressed as $C = f(t)$, and increased markedly for $\alpha \gg 0$. In the first stage, a pronounced increase in C is produced, and subsequently, due to the increasing nitrogen supersaturation in the liquid at the α-Si_3N_4/liquid interface, nucleation of the β-phase is promoted, and therefore C will increase moderately being approximately asymptotic to a limiting value as

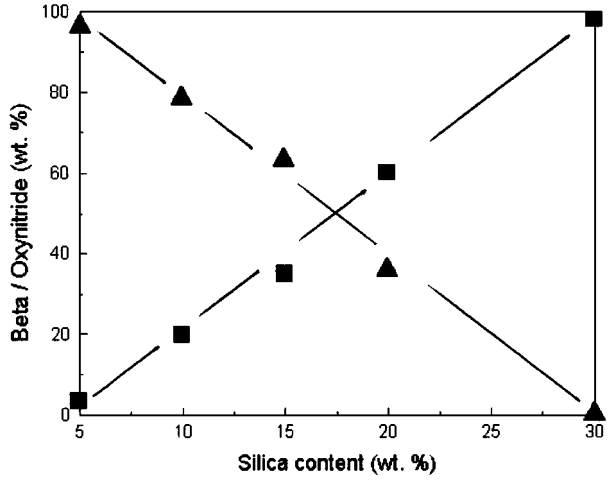

Figure 6 Variation of (▲) β-Si_3N_4 and (■) Si_2N_2O with the silica content, after HIPing at 1900 °C, 150 MPa during 60 min.

α approaches zero. It is clear that as $\alpha \rightarrow 0$, C must decrease, but in a non-linear fashion because, as the quantity of β-Si_3N_4 increases, the points of nucleation are less frequent and compositional gradients in the liquid are reduced. Analysing the results as a function of the quantity of SiO_2 added, it is apparent that for a given time, as expected from the phase diagram, the closer the composition (mol %) to the stoichiometric ratio ($Si_3N_4/SiO_2 = 1$), the more Si_2N_2O is observed. In contrast, if the composition of the powder mix is closer to the Si_3N_4-rich region, the precipitation of β-Si_3N_4 is favoured (Fig. 6).

The evolution of the different crystalline phases can also be followed through microstructural development, and is most clearly marked in the samples corresponding to the extreme compositions. Fig. 7 shows the changes in the microstructure with temperature for specimens of Si_3N_4–30% SiO_2. At 1750 °C (Fig. 7a) Si_2N_2O is not observed, but a large number of equiaxed α-Si_3N_4 grains (35 vol%) and some elongated β-Si_3N_4 grains (5 vol %) are seen to be embedded in a high volume fraction of intergranular phase (54 vol %).

At 1850 °C (Fig. 7b) the volume fraction of intergranular phase is less than before (20 vol %), but the number of elongated grains (with a somewhat lower aspect ratio) has increased (70 vol %). From the electron diffraction patterns obtained it was deduced that some of these elongated grains (generally those showing twins aligned along the long axis of the grains) correspond to Si_2N_2O.

Finally, at 1900 °C only Si_2N_2O grains are observed, the intergranular phase is present in only minor amounts along grain boundaries and at triple points, and the Si_2N_2O grains are much more equiaxed, showing a wide distribution of sizes (Fig. 7c).

The composition with the lowest content of SiO_2 (5%) is only fully dense at 1900 °C. At this temperature, a complete transformation to β-Si_3N_4 has taken place. The grains are equiaxed, presenting a large number of contacts between grains and good shape accommodation (Fig. 8).

Additions of Y_2O_3 produce an important accelerating effect on, both, transformation and densification.

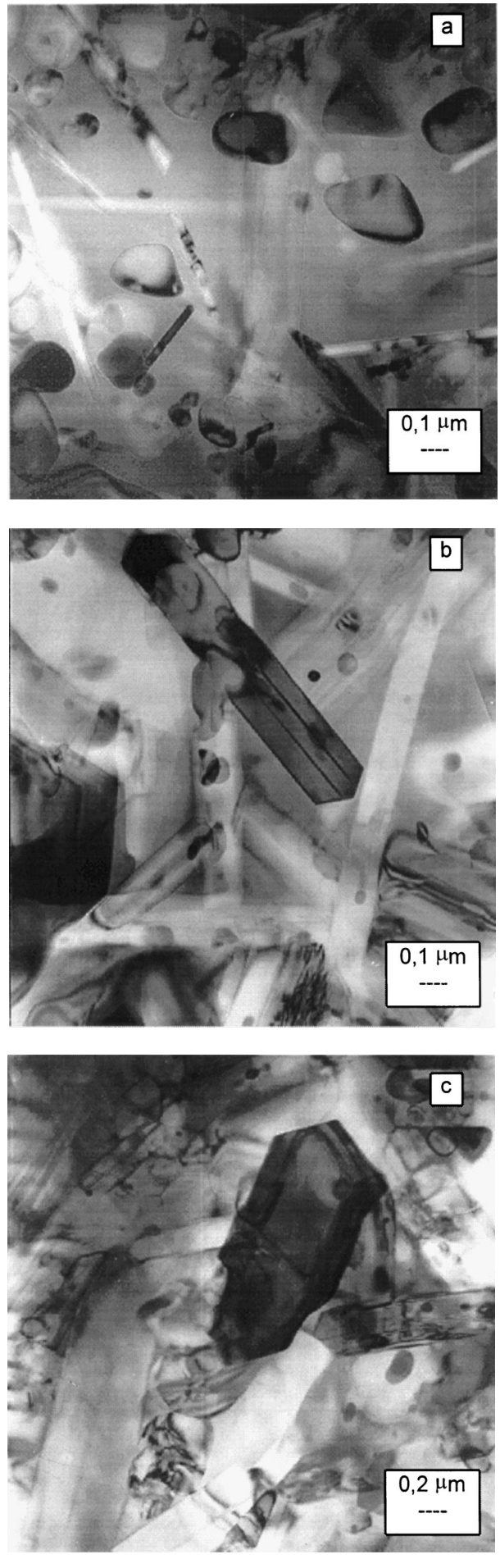

Figure 7 Microstructural evolution as a function of sintering temperature for Si_3N_4 + 30% SiO_2 samples: (a) 1750 °C, (b) 1850 °C and (c) 1900 °C.

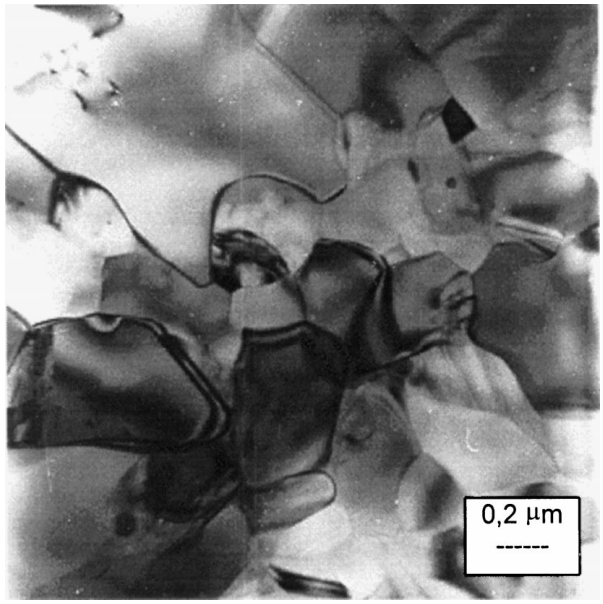

Figure 8 Transmission electron micrograph of a specimen of Si_3N_4 containing 5% SiO_2 after HIPing at 1900 °C, 150 MPa for 60 min.

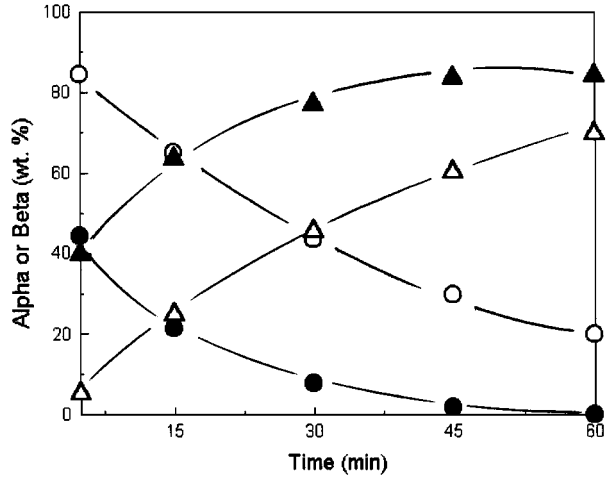

Figure 9 (○, ●) α-Si_3N_4 and (△, ▲) β-Si_3N_4 concentration as a function of holding time for samples of (○, △) Si_3N_4–3% Y_2O_3–2% SiO_2 and (●, ▲) Si_3N_4–6% Y_2O_3–4% SiO_2.

In this case, Y_2O_3 addition creates less viscous liquid phases with a lower melting point, which allows faster transport of material by diffusion and consequently higher densities. Additionally, Y_2O_3 additions change the composition of the liquid at the sintering temperature in the Si_3N_4–SiO_2–Y_2O_3 system. Precipitation of the silicon oxynitride ceases and β-Si_3N_4 is favoured.

The dissolution–diffusion-precipitation mechanisms combined with rearrangement and liquid redistribution with porosity filling, assisted by the smaller viscosity of the liquid phase, allow high densities values to be reached at relatively low temperatures.

In contrast to the Si_3N_4–SiO_2 system, Table II shows that in the Si_3N_4–Y_2O_3–SiO_2 system, the amorphous phase concentration remains constant with time, thus indicating that the α-Si_3N_4 that is dissolved in the liquid phase reprecipitates as β-Si_3N_4.

The measurements summarised in Table II indicate that the dissolution rate of α-Si_3N_4 decreases as the amount of β-Si_3N_4 increases (Fig. 9).

The dissolution rate of the α-phase will be at each moment proportional to its concentration, and this can be expressed as

$$\frac{d\alpha}{dt} = -k\alpha \qquad (2a)$$

which on integration gives

$$\ln \alpha = \ln \alpha_0 - kt \qquad (2b)$$

Such a relationship establishes, for the two compositions studied, that the dissolution of the α-phase follows a first-order reaction. The dissolution rate depends not only on the concentration of the α-phase, but also on the composition and amount of vitreous phase as given by k. The quantity and viscosity of the liquid phase will determine the extent to which compositional gradients and the nitrogen supersaturation in the α-Si_3N_4/liquid interface are maintained. The composition of the resulting liquid phase is very important for α-Si_3N_4 dissolution, in this case, as the two discussed compositions fall in the same compatibility triangle, the liquid phases formed will have the same composition. Therefore, the larger amount of liquid present during sintering in the 6% Y_2O_3–4% SiO_2 composition will cause the transformation to take place earlier and quicker. It seems reasonable to expect that the more liquid that is present, the longer it will take to reach the degree of supersaturation necessary for the precipitation of β-Si_3N_4, but at the studied temperature this is not reached, because for $t = 5$ min the quantity of α-Si_3N_4 that has transformed into β-Si_3N_4 is significant. In these conditions, i. e. once the dissolution–diffusion–precipitation process has reached its steady state, the increased quantity of liquid will lead to an increased fraction of β-Si_3N_4 precipitating. It is worth recalling that in this system

TABLE II α-Si_3N_4, β-Si_3N_4 and intergranular phase concentration as a function of the holding time

Time (min)	Si_3N_4–3 wt % Y_2O_3–2 wt % SiO_2			Si_3N_4–6 wt % Y_2O_3–4 wt % SiO_2		
	α	β	Vitreous phase	α	β	Vitreous phase
5	84.4	5.1	10.5	44.3	39.7	16.0
15	65.0	24.7	10.3	21.2	63.4	15.4
30	43.2	45.3	11.5	7.6	76.8	15.6
45	29.7	60.3	10.2	1.7	83.3	15.0
60	19.7	69.8	10.5	0	84.0	16.0

the liquid-phase concentration remains constant during the transformation process. The constancy of the intergranular phase concentration for all the holding times at the sintering temperature is a sufficient and necessary condition for the transformation in this system to be a process whose kinetics are controlled by the dissolution of the α-Si_3N_4 in the liquid phase. If the dissolved α-Si_3N_4 had not diffused and precipitated as β-Si_3N_4, there would be some time intervals in which an increase in the intergranular phase would be observed.

The constancy of C leads to

$$\frac{d\beta}{dt} = -\frac{d\alpha}{dt} \tag{3}$$

and because $\alpha + \beta = 1 - C$ then using Equation 2b this gives

$$\frac{d\beta}{dt} = k\alpha$$
$$= k(1 - C - \beta) \tag{4}$$

$$\beta(t) = \beta_i + \alpha_0(1 - e^{-kt}) \tag{5}$$

Equation 5 indicates that β-Si_3N_4 formation is determined by nucleation and growth, the kinetics of which can be represented by Avrami's equation. The transformation can also be described by the Johnson–Mehl equation for nucleation and growth processes [10]

$$\beta(t) = 1 - \exp(-bt^n) \tag{6}$$

where b is a constant that depends on the nucleation and growth rates and is therefore very sensitive to temperature and n is the Avrami exponent which, if no changes in nucleation mechanism occur, is independent of temperature.

Equation 6 implies a linear relationship between $\ln[-\ln(1 - \beta)]$ and $\ln t$; the curves obtained for the experimental data can be seen in Fig. 10.

The values of b and n obtained by fitting the experimental data are presented in Table III.

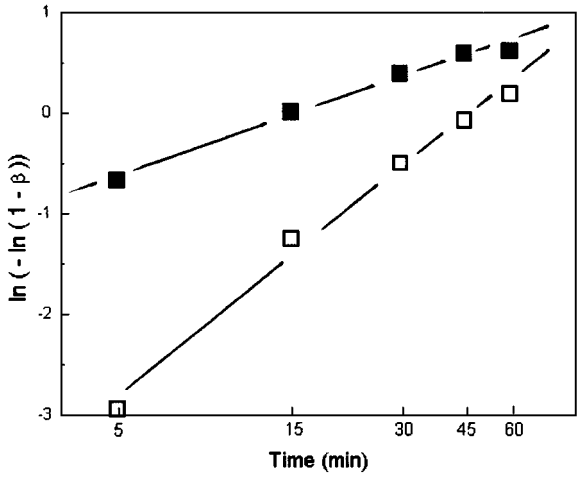

Figure 10 Linear relationship between $\ln[-\ln(1 - \beta)]$ and $\ln t$ for (□) Si_3N_4–3% Y_2O_3–2% SiO_2 and (■) Si_3N_4–6% Y_2O_3–4% SiO_2.

TABLE III Exponent and constant of the Avrami equation obtained by fitting of experimental points

Composition	b	n
Si_3N_4–$3Y_2O_3$–$2SiO_2$	8×10^{-3}	1.3
Si_3N_4–$6Y_2O_3$–$4SiO_2$	224×10^{-3}	0.6

If the values of n obtained experimentally are compared with those reported [11], it is clear that in the 3% Y_2O_3 sample particles have a considerable initial volume. This fact would be in agreement with the hypothesis supported by Petzow and Hoffman [12]. These researchers assert that nucleation, either homogeneously or heterogeneously, does not influence microstructural development and that only pre-existent β-Si_3N_4 particles seem to grow. In contrast to their statement, it can be argued that the same microstructure is achieved if

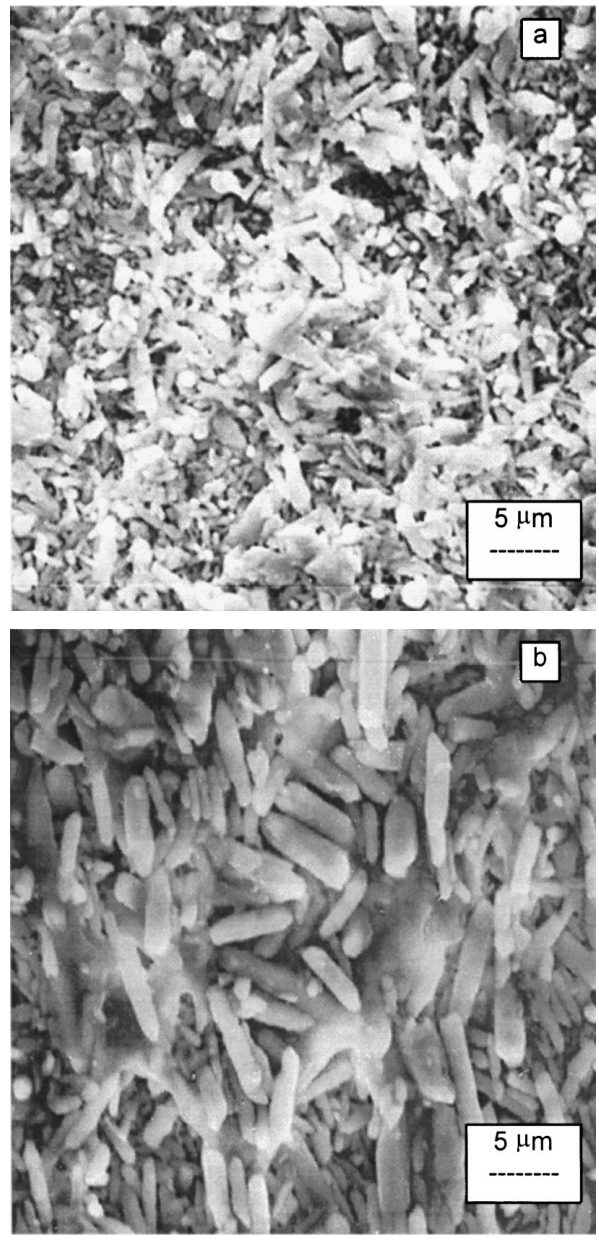

Figure 11 Scanning electron micrographs of Si_3N_4–6% Y_2O_3–4% SiO_2 HIPed at 1750 °C for different holding times under an argon pressure of 150 MPa: (a) 15 min, and (b) 60 min.

small grains of β-Si_3N_4 nucleated on the pre-existent grains, are outgrown by others ones during the growth process. Contrary to the Petzow and Hoffman hypothesis, Gómez *et al.* [13] have observed the nucleation of β-Si_3N_4 grains from α-Si_3N_4 during SiC nitridation. In this case, the nucleation of the β-phase occurs without pre-existent β-Si_3N_4 grains.

In the case of the composition with 6% Y_2O_3 the value of n is located between that corresponding to needle enlargement ($n = 1$) and large plate enlargement ($n = 0.5$).

Taking into account that the determined values are approximate and that the β-Si_3N_4 grains are needle shaped, it could be expected that the n values obtained experimentally correspond to appropriate condition of needle growth. Microstructural observations confirm this hypothesis, and thus in the micrograph (Fig. 11) it can be appreciated that for a holding time of 15 min. (β-$Si_3N_4 \sim 63$ wt %) needles with a 1μm diameter and a length of 4–5 μm are obtained (Fig. 11a), while for 60 min (Fig. 11b) the diameter is approximately doubled in size (2–2.5 μm) whilst the length remains practically constant.

4. Conclusions

1. It has been observed that during the hot isostatic pressing of samples in the Si_3N_4–SiO_2 system, the dissolution rate of α-Si_3N_4 is constant and the quantity of intergranular phase increases with time in the range 1700–1800 °C. This indicates that the process which controls the transformation kinetics in this system is not the dissolution of α-Si_3N_4.

2. The formation of Si_2N_2O is a reaction that competes with the precipitation of β-Si_3N_4. The closer the composition is (in mole %) to the stoichiometric ratio ($Si_3N_4/SiO_2 = 1$), the more Si_2N_2O is observed.

3. The addition of Y_2O_3 has an important accelerating effect on both transformation and densification. The liquid phase formed in this system is less viscous and therefore material transport mechanisms proceed faster.

4. In the Si_3N_4–Y_2O_3–SiO_2 system the quantity of intergranular phase remains constant with time and the dissolution rate is proportional to α-Si_3N_4 concentration. In this system the transformation kinetics are controlled by the dissolution of α-Si_3N_4.

5. By varying the Y_2O_3/SiO_2 ratio, densification and $\alpha \rightarrow \beta$ transformation can be controlled independently, so that the complete range of samples can be obtained, from dense samples showing no transformation, through to porous samples with complete transformation.

Acknowledgement

S. Ordoñez acknowledges the financial support from Dirección de Investigaciones Científicas y Tecnológicas (DICYT), Universidad de Santiago de Chile.

References

1. G. ZIEGLER, J. HEINRICH and G. WÖTTING, *J. Mater. Sci.* **22** (1987) 3041.
2. T. EKSTRÖM and M. NYGREN, *J. Am. Ceram. Soc.* **75** (2) (1992) 259.
3. F. F. LANGE, *Int. Metal. Rev.* **1** (1980) 1.
4. S. HAMPSHIRE and K. JACK, in "Special Ceramics," Vol. 7, edited by Taylor and Popper (British Ceramic Society, Stoke-on-Trent, (1981) p. 37.
5. C. BOBERSKI, H. BESTGEN and R. HAMMINGER, *J. Eur. Ceram. Soc.* **9** (1992) 95.
6. Z. PANEK and M. PROKESOVA, *J. Mater. Sci.* **25** (1990) 3709.
7. N. BUTLER, J. WOODTHORPE, I. ITURRIZA and F. CASTRO, US Pat. 5089 197 18 February 1992.
8. B.D. CULLITY, in "Elements of X-ray diffraction", 2nd Edn (Addison-Wesley, Reading, MA, 1978).
9. I. ITURRIZA and F. CASTRO, *J. Mater. Sci. Lett.* **9** (1990) 600.
10. W. A. JOHNSON and R. F. MEHL, *Trans. AIME* **1135** (1939) 416.
11. J. W. CHRISTIAN, in "Transformations of metals and alloys" (Pergamon Press, New York, 1965) p. 489.
12. G. PETZOW and M. J. HOFFMAN, "Materals Science Forum", Vols 113–115 (Trans. Tech. Publications, Switzerland, 1993) p. 91.
13. E. GÓMEZ, T. GÓMEZ-ACEBO, J. ECHEBERRÍA, I. ITURRIZA and F. CASTRO, *J. Eur. Ceram. Soc.* **14** (1994) p. 411.

Received 9 November 1997
and accepted 23 July 1998